A New Class of *C. elegans* synMuv Genes Implicates a Tip60/NuA4-like HAT Complex as a Negative Regulator of Ras Signaling

Craig J. Ceol and H.R. Horvitz*
Howard Hughes Medical Institute
Department of Biology, 68-425
Massachusetts Institute of Technology
Cambridge, Massachusetts 02139

Summary

The class A and class B synMuv genes are functionally redundant negative regulators of a Ras signaling pathway that induces *C. elegans* vulval development. A number of class B synMuv genes encode components of an Rb and histone deacetylase complex that likely acts to repress transcription of genes required for vulval induction. We discovered a new class of synMuv genes that acts redundantly with both the A and B classes of genes in vulval cell-fate determination. These new class C synMuv genes encode TRRAP, MYST family histone acetyltransferase, and Enhancer of Polycomb homologs, which form a putative *C. elegans* Tip60/NuA4-like histone acetyltransferase complex. A fourth gene with partial class C synMuv properties encodes a homolog of the mammalian SWI/SNF family ATPase p400. Our findings indicate that the coordinated action of two chromatin-modifying complexes, one with histone deacetylase and the other with histone acetyltransferase activity, is important in regulating Ras signaling and specifying cell fates during *C. elegans* development.

Introduction

Protein complexes that remodel and chemically modify chromatin have been isolated using cellular fractionation techniques, and roles for many of these complexes in transcription and other cellular processes have been identified by biochemical and genetic studies (Roth et al., 2001; Becker and Horz, 2002). However, little is known about how these complexes and, more generally, how alterations in chromatin structure contribute to animal development. Studies of Ras-mediated vulval induction in the nematode *Caenorhabditis elegans* have begun to address this issue.

In the wild-type *C. elegans* hermaphrodite, the vulva is formed by the 22 descendants of three ectodermal blast cells, P5.p, P6.p, and P7.p (Sulston and Horvitz, 1977). During larval development, these cells receive an inductive signal from the nearby gonadal anchor cell (Sulston and White, 1980; Kimble, 1981). P6.p responds by dividing to generate eight descendants, while P5.p and P7.p generate seven descendants each. P5.p, P6.p, and P7.p are said to adopt vulval fates. Although the flanking cells, P3.p, P4.p, and P8.p, are competent to adopt vulval fates, they do not receive sufficient inductive signal and consequently adopt nonvulval fates, typically dividing once to generate descendants that fuse

with the syncytial hypodermis (Sternberg and Horvitz, 1986). Vulval induction requires the activity of a conserved Ras signaling pathway (reviewed by Sternberg and Han, 1998). Mutations that disable *let-60* Ras and other genes in this pathway result in a vulvaless (Vul) phenotype in which all six P(3–8).p cells adopt nonvulval cell fates (Sulston and Horvitz, 1981; Beitel et al., 1990; Han and Sternberg, 1990). Mutations that overactivate this pathway, for instance mutations that create the same G13E substitution found in oncogenic forms of human Ras, cause a multivulva (Muv) phenotype that is characterized by hyperinduction in which more than three P(3–8).p cells adopt vulval cell fates (Beitel et al., 1990).

Loss-of-function mutations in the synthetic multivulva (synMuv) genes can also cause a Muv phenotype. On the basis of genetic interactions, the synMuv genes are grouped into two classes, A and B (Ferguson and Horvitz, 1989). For an animal to be Muv, it must carry a mutation in both a class A and a class B gene. These genetic interactions led to the proposal that classes A and B encode two functionally redundant genetic pathways that negatively regulate vulval development. The class B synMuv genes include *lin-35*, which encodes a homolog of the mammalian Rb tumor suppressor protein (Lu and Horvitz, 1998), and *efl-1* and *dpl-1*, which encode homologs of E2F and DP DNA binding transcription factors, respectively (Ceol and Horvitz, 2001). LIN-35 Rb, EFL-1, and DPL-1, together with other class B synMuv proteins, are proposed to recruit the histone deacetylase HDA-1 to promoters to regulate the transcription of genes important for vulval development (Lu and Horvitz, 1998; Ceol and Horvitz, 2001). LET-418, a homolog of Mi-2 ATP-dependent chromatin remodeling enzymes, and LIN-53, a homolog of the RbAp46 and RbAp48 proteins that are found in many chromatin remodeling complexes, are also class B synMuv proteins (Lu and Horvitz, 1998; Solari and Ahringer, 2000; von Zelewsky et al., 2000). Mi-2 as well as HDAC1 and HDAC2, which are mammalian class I histone deacetylases similar to HDA-1, and RbAp46 and RbAp48 are components of the Nucleosome Remodeling Deacetylase (NuRD) complex. The involvement of HDA-1, LET-418, and LIN-53 suggests that regulation of chromatin structure, possibly by a *C. elegans* counterpart of the NuRD complex, is important for vulval cell-fate specification in *C. elegans*.

In this study, we report the identification of a distinct class of genes, termed the class C synMuv genes, that negatively regulate vulval induction. Loss-of-function mutations in class C synMuv genes alone cause mild vulval defects and synergize with either class A or class B mutations to produce more severe vulval and other developmental defects. The four genes in this new class, *trr-1*, *mys-1*, *epc-1*, and *ssl-1*, encode homologs of the transcriptional coactivator TRRAP, the MYST family histone acetyltransferases TIP60 and Esa1p, the *Drosophila* Enhancer of Polycomb [E(Pc)] protein, and the SWI/SNF family ATPase p400, respectively. Because TRRAP, E(Pc), and p400 proteins have been copurified with histone acetyltransferases (Allard et al., 1999; Galarneau

*Correspondence: horvitz@mit.edu

et al., 2000; Ikura et al., 2000; Fuchs et al., 2001; Frank et al., 2003), we propose that a multisubunit chromatin remodeling histone acetyltransferase complex acts to specify vulval cell fates in *C. elegans*. Since the class C synMuv genes function redundantly with the class B synMuv genes, both histone acetyltransferase and deacetylase activities may be required to negatively regulate Ras-mediated vulval development.

Results

trr-1 Mutations Interact with Class A and Class B synMuv Mutations

We performed a genetic screen for synMuv mutants in a *lin-15A(n767)* background (C.J.C., F. Stegmeier, M. Harrison, and H.R.H., unpublished data) and identified six mutations that mapped to the same linkage group, failed to complement each other, and defined the gene *trr-1* (this gene name will be explained below). To more precisely quantitate the Muv phenotype of *trr-1; lin-15A* strains, we scored the numbers of P(3–8).p cells per animal that adopted vulval cell fates. Whereas only three cells typically adopt vulval cell fates in wild-type animals, more than four cells adopted vulval cell fates in each of the *trr-1; lin-15A* mutants (Table 1A). In each of the *trr-1; lin-15A* strains, this abnormality in vulval cell fates was recessive and temperature sensitive (Table 1A; data not shown). The recessive nature of the phenotype caused by these mutations is consistent with the possibility that all of them cause a loss of gene function.

To determine if *trr-1* interacts with other class A synMuv genes, we constructed a strain carrying *trr-1(n3712)* and a mutation in the class A synMuv gene *lin-38*. In these double mutant animals, more than four P(3–8).p cells adopted vulval cell fates (Table 1A), suggesting that *trr-1* functions in parallel not only to *lin-15A* but more generally to the set of class A synMuv genes.

We also separated *trr-1(n3712)* and the other *trr-1* mutations from any other synMuv mutations. Nearly all class A and class B synMuv single mutants adopt a wild-type pattern of P(3–8).p fates (data not shown). However, *trr-1* adults displayed a weakly penetrant phenotype of ectopic vulval cell fates (Table 1B). By examining the cell fates adopted by individual P(3–8).p cells in L4 animals, we determined that the vulval cell-fate transformations of *trr-1* single mutants always affected P8.p. Specifically, in 38 of 38 *trr-1* single mutants with ectopic vulval cell fates, P8.p expressed a vulval fate whereas P3.p and P4.p did not. In addition to ectopic vulval cell-fate transformations, all *trr-1* mutations caused slow growth and sterility; a few mutant animals produced a small number of eggs (<10, as compared to about 300 for the wild-type), all of which died during embryogenesis.

To determine if *trr-1* interacts with class B synMuv genes, we constructed double mutant strains containing *trr-1(n3712)* and mutations of class B synMuv genes. Interestingly, double mutants combining *trr-1(n3712)* with mutations of *lin-15B*, *lin-35* Rb, *lin-36*, *lin-37*, and *dpl-1* showed a synergistic increase in the penetrance of P8.p transformation (Table 1C). In addition to the increase in P8.p transformation, occasional ectopic transformations of P3.p and P4.p occurred (data not shown). If the severity of a defect in a double mutant exceeds that of either single mutant, then two genes likely do not act in a linear genetic pathway, assuming that at least one of the mutations is a null allele. Since *lin-15B(n744)*, *lin-35(n745)*, *lin-36(n3096)*, *lin-37(n758)*, and *dpl-1(n3316 RNAi)* are strong loss-of-function and likely null mutations of their corresponding genes (Lu and Horvitz, 1998; Lu, 1999; Thomas and Horvitz, 1999; Ceol and Horvitz, 2001; our unpublished data), these results indicate that *trr-1* functions redundantly with at least a subset of class B synMuv genes (see also Supplemental Data at http://www.developmentalcell.com/cgi/content/full/6/4/563/DC1).

trr-1 Encodes a Protein Similar to Mammalian TRRAP

We mapped *trr-1* to a small region of LGII (Figure 1A) and cloned the gene using transformation rescue with cosmid C47D12 (see Experimental Procedures). To confirm the identity of *trr-1*, we obtained a partial cDNA and found that RNAi using dsRNA derived from this cDNA led to extra vulval cell fates in *lin-15A* and *lin-38* mutant backgrounds (Table 1A). *trr-1(RNAi)* also led to extra vulval cell fates in the class A synMuv *lin-8* and *lin-56* mutant backgrounds, further confirming that *trr-1* acts in parallel to the class A synMuv genes. *trr-1* corresponds to the predicted gene C47D12.1. As determined by RT-PCR and 5′ RACE, the *trr-1* gene consists of 22 exons, four of which are alternatively spliced (Figure 1A). Since the sites of alternative splicing are separated by only six or nine nucleotides, the most exclusive (4054 amino acids) and inclusive (4064 amino acids) predicted isoforms differ only slightly in size.

The predicted TRR-1 proteins are similar to the mammalian myc-associated protein TRRAP (transformation/transcription domain-associated protein) and its yeast homolog Tra1p throughout most of their lengths (McMahon et al., 1998; Saleh et al., 1998). TRRAP and Tra1p are similarly large proteins, of 3828 and 3744 amino acids, respectively. The largest predicted TRR-1 isoform is 25 percent identical to TRRAP and 19 percent identical to Tra1p. TRR-1, TRRAP, and Tra1p share limited regions of similarity with other proteins. One region, located at the carboxy terminus, is similar to the catalytic domains of ATM, PI-3, and other kinases (Figure 1B). However, the DXXXXN and DFG motifs critical for kinase activity (Hunter, 1995) are not present in TRR-1, TRRAP, or Tra1p. Instead of having an enzymatic function, this domain of TRRAP has been proposed to mediate protein-protein interactions (McMahon et al., 1998). Another motif, the FAT domain, is located in the carboxy-terminal half of the protein (Figure 1B) and is also found in FRAP and ATM kinases. The biochemical function of this domain is unknown. All six *trr-1* mutations introduce nonsense codons (Figure 1B). *trr-1(n3630)*, *trr-1(n3637)*, and *trr-1(n3712)* introduce amber stop codons, and we observed that the sterility associated with these alleles was greatly reduced by the *sup-5(e1464)* informational suppressor tRNA mutation: *trr-1(n3630)*, *trr-1(n3637)*, and *trr-1(n3712)* strains were 100% sterile, but in double mutants with *sup-5(e1464)*, sterility was suppressed to 0%, 3.3%, and 7.1%, respectively (n = 30 for each strain). This suppression, along with the partially penetrant sterility caused by *trr-1(RNAi)* (data not shown), shows that the sterility observed in *trr-1* mutant strains is caused by a loss of *trr-1* function.

Table 1. *trr-1* Mutants Have Ectopic Vulval Cell Fates

Genotype	Temp (°C)	Average # P(3–8).p Vulval Fates ± SE	% Animals with >3 Vulval Fates	n
A. *trr-1* Interactions with *synmuvA* Mutations				
wild-type	20	3.00 ± 0	0	31
lin-15A(n767)	20	3.00 ± 0	0	24
lin-38(n751)	20	3.00 ± 0	0	27
trr-1(n3630); lin-15A(n767)	20	4.52 ± 0.15	82	45
trr-1(n3637); lin-15A(n767)	20	4.52 ± 0.14	83	54
trr-1(n3704); lin-15A(n767)	20	4.20 ± 0.13	79	43
trr-1(n3708); lin-15A(n767)	20	4.71 ± 0.14	92	36
trr-1(n3709); lin-15A(n767)	20	4.81 ± 0.13	95	39
trr-1(n3712); lin-15A(n767)	20	4.07 ± 0.12	74	54
trr-1(n3704)/+; lin-15A(n767)	20	3.00 ± 0	0	41
trr-1(n3712)/+; lin-15A(n767)	20	3.00 ± 0	0	30
trr-1(n3712) lin-38(n751)	20	4.14 ± 0.23	79	14
trr-1(RNAi); lin-15A(n767)	20	5.60 ± 0.08	100	44
trr-1(RNAi) lin-38(n751)	20	5.66 ± 0.08	100	32
trr-1(RNAi); lin-8(n2731)	20	5.69 ± 0.08	100	35
trr-1(RNAi); lin-56(n2728)	20	5.55 ± 0.14	97	31
wild-type	15	3.00 ± 0	0	29
lin-15A(n767)	15	3.00 ± 0	0	32
trr-1(n3704); lin-15A(n767)	15	3.13 ± 0.05	21	24
trr-1(n3712); lin-15A(n767)	15	3.06 ± 0.03	13	32
wild-type	25	3.00 ± 0	0	36
lin-15A(n767)	25	3.02 ± 0.02	3.6	28
trr-1(n3704); lin-15A(n767)	25	5.87 ± 0.06	100	38
trr-1(n3712); lin-15A(n767)	25	5.47 ± 0.14	100	17
B. *trr-1* Single Mutants				
wild-type	20	3.00 ± 0	0	31
trr-1(n3630)	20	3.03 ± 0.02	6.1	33
trr-1(n3637)	20	3.08 ± 0.04	13	30
trr-1(n3704)	20	3.01 ± 0.01	2.6	39
trr-1(n3708)	20	3.05 ± 0.03	8.1	37
trr-1(n3709)	20	3.03 ± 0.02	6.3	32
trr-1(n3712)	20	3.10 ± 0.03	13	89
trr-1(RNAi)	20	3.09 ± 0.05	13	32
wild-type	15	3.00 ± 0	0	29
trr-1(n3704)	15	3.08 ± 0.05	12	26
trr-1(n3712)	15	3.06 ± 0.03	12	25
wild-type	25	3.00 ± 0	0	36
trr-1(n3704)	25	3.04 ± 0.03	3.9	51
trr-1(n3712)	25	3.07 ± 0.03	13	48
C. *trr-1* Interactions with *synmuvB* Mutations				
wild-type	20		0	31
lin-15B(n744)	20		0	20
lin-35(n745)	20		0	48
lin-36(n3096)	20		0	28
lin-37(n758)	20		0	32
dpl-1(n3316 RNAi)	20		8.1	37
trr-1(n3712)	20		13	89
trr-1(n3712); lin-15B(n744)	20		50	38
lin-35(n745); trr-1(n3712)	20		64	41
trr-1(n3712); lin-36(n3096)	20		31	29
trr-1(n3712); lin-37(n758)	20		55	20
dpl-1(n3316 RNAi) trr-1(n3712)	20		32	34

The number of P(3–8).p vulval fates was scored as described in the Experimental Procedures. *trr-1* mutant homozygotes were recognized as non-Gfp progeny of *trr-1/mIn1[dpy-10(e128) mIs14]* heterozygous parents. *dpl-1* encodes the sole DP family protein in *C. elegans*, and loss of *dpl-1* function is predicted to abrogate all DP/E2F function in the organism. To approximate a null condition for *dpl-1*, we combined the deletion mutation *dpl-1(n3316)*, which eliminates zygotically provided *dpl-1* activity and causes sterility, with *dpl-1(RNAi)*, which strongly reduces maternally provided *dpl-1* activity (Ceol and Horvitz, 2001).

TRR-1 Is Expressed Broadly and Is Localized to Nuclei

We generated antibodies to determine the expression pattern and subcellular localization of the TRR-1 protein. These antibodies were specific for TRR-1, as they did not detect protein in *trr-1(RNAi)* adults (data not shown). In whole-mount stainings of wild-type animals, TRR-1 was detected in the nuclei of one-cell and subsequent stage embryos (Figures 1C and 1F). TRR-1 was present in weakly detectable levels in somatic nuclei of larvae
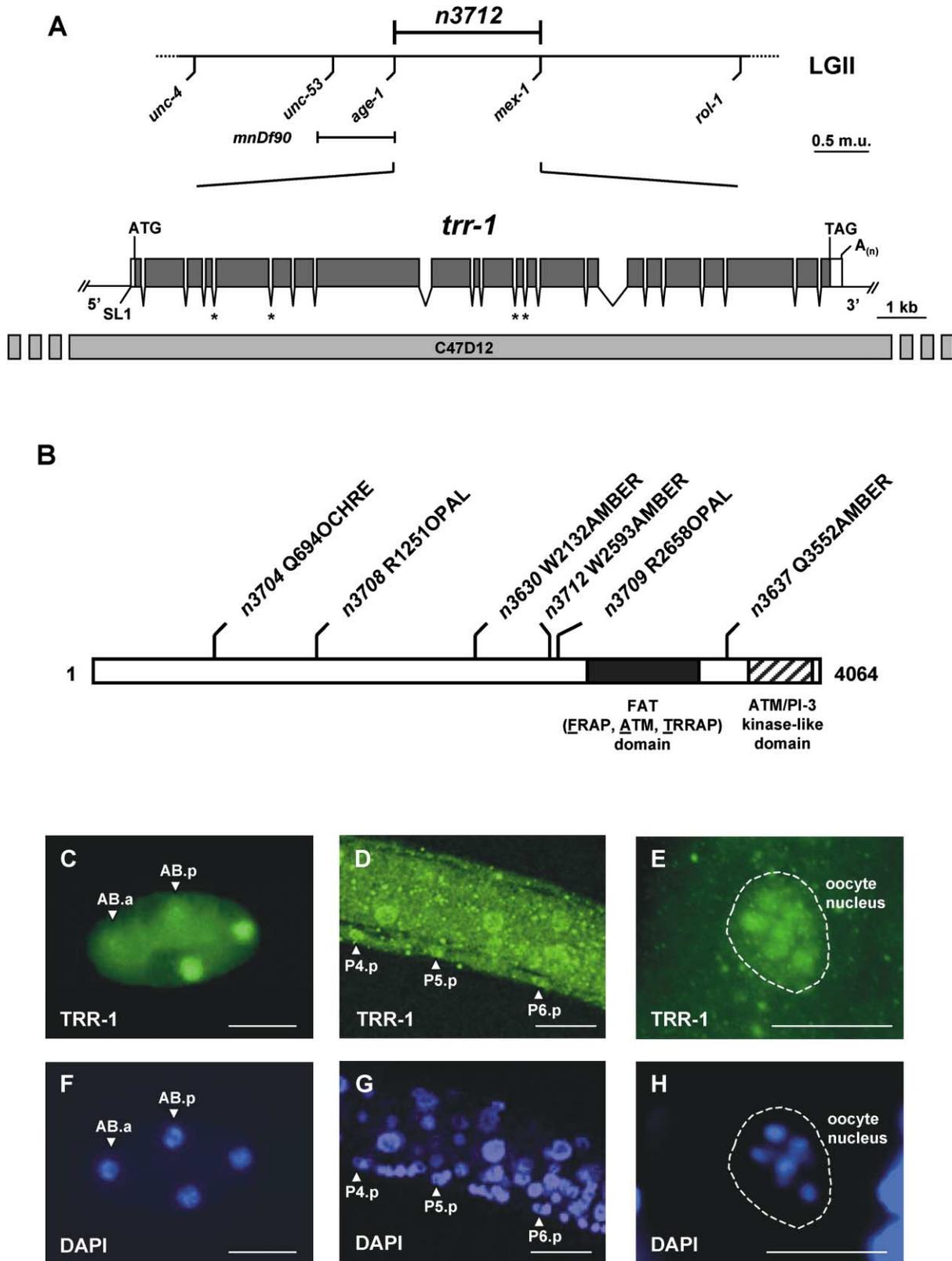
Figure 1. *trr-1* Cloning and Expression

(A) The genetic map position of *trr-1(n3712)* is shown above. The *trr-1* gene structure as derived from cDNA and genomic sequences is indicated below. Shaded boxes indicate coding sequence and open boxes indicate 5′ and 3′ untranslated regions. Predicted translation initiation and termination codons and the poly(A) tail are shown. Positions of alternative splicing are indicated by asterisks. In all cases, the

and adults. Among the nuclei expressing TRR-1 were those of P(3–8).p (Figures 1D and 1G). TRR-1 was readily detectable in germ nuclei of larvae and adults. During the pachytene (data not shown) and diakinesis (Figures 1E and 1H) stages of meiosis I, as observed in syncytial germ nuclei and cellularized oocytes, respectively, TRR-1 was localized to condensed chromosomes. However, TRR-1 was not specifically localized to condensed mitotic chromosomes of early-stage embryos (Figures 1C and 1F).

The Muv Phenotype of *trr-1* Mutants Requires *let-60* Ras Pathway Activity

To determine if Ras pathway activity is required for the *trr-1* mutant phenotype, we constructed strains in which the functions of *trr-1*, *lin-15A*, and a Ras pathway gene were reduced or eliminated. The lack of vulval cell fates caused by *let-23* receptor tyrosine kinase and *let-60* Ras mutations was epistatic to the ectopic vulval cell fate phenotype caused by *trr-1* and *lin-15A* loss of function (Table 2). This result indicates that Ras pathway activity is required to produce the *trr-1; lin-15A* Muv phenotype. It is possible that class A synMuv genes such as *lin-15A* but neither *trr-1* nor class B synMuv genes require Ras pathway activity for a Muv phenotype. To investigate this possibility, we constructed *let-23 trr-1; lin-15B* and *trr-1; let-60; lin-15B* triple mutants. The low numbers of vulval cell fates in these triple mutants indicate that the *trr-1; lin-15B* Muv phenotype is also dependent on Ras pathway activity. Taken together, these results indicate that at least two of the three classes of synMuv genes (class A, class B, and *trr-1*) require Ras pathway activity for a Muv phenotype.

By contrast, *trr-1; lin-3; lin-15A* mutants had a Muv phenotype, with P(3–8).p cells all adopting vulval cell fates (Table 2). *lin-3* encodes an EGF-like protein that is produced by the gonadal anchor cell and can act non-cell autonomously to stimulate Ras pathway activity in P(5–7).p (Hill and Sternberg, 1992). These findings suggest that *lin-3*-independent Ras pathway activity, in the background of *trr-1* and *lin-15A* losses of function, is necessary for the expression of vulval cell fates by P(3–8).p. The number of vulval cell fates in *trr-1; lin-3; lin-15B* triple mutants was between that of *lin-3* single and *trr-1; lin-15B* double mutants. We observed a similar number in *lin-3; lin-15B* double mutants. It is possible

that the synthetic interaction we have found between *trr-1* and *lin-15B* is too small to be observed in a *lin-3* background. Alternatively, *trr-1* and *lin-15B* may simply not synthetically interact in their suppression of *lin-3*. In either case, *lin-3*-independent Ras pathway activity is clearly necessary for vulval cell fates in a *trr-1; lin-15B* mutant background.

Mutants Deficient in *mys-1*, which Encodes a MYST Family Histone Acetyltransferase, Display Abnormalities Similar to Those of *trr-1* Mutants

TRRAP and Tra1p are components of biochemically purified multisubunit histone acetyltransferase (HAT) complexes (Allard et al., 1999; Brown et al., 2000; Ikura et al., 2000). These complexes are distinguished by their HAT subunits: the mammalian TFTC and p/CAF and the yeast SAGA complexes contain Gcn5 family HATs, whereas the mammalian Tip60 and the yeast NuA4 complexes contain MYST family HATs. TRR-1 may function in a complex similar to one or more of these HAT complexes to regulate the specification of vulval cell fates.

To address this issue, we inactivated genes encoding *C. elegans* homologs of HATs using RNAi and looked for abnormalities similar to those caused by loss of *trr-1* (Table 3). Inactivation of a Gcn5 homolog *Y47G6A.6* or of the MYST family genes *C34B7.4* and *K03D10.3* in a class A synMuv background had no effect on vulval development. Inactivation of a third MYST family gene, *R07B5.8*, produced a vulvaless (Vul) phenotype in either a *lin-15A* or otherwise wild-type genetic background. We suspect this defect is a consequence of the lack of a functional anchor cell, as the morphology of the somatic gonad in *R07B5.8(RNAi)* mutants is severely disrupted (data not shown).

By contrast, inactivation of a MYST family gene we have named *mys-1* produced a highly penetrant Muv phenotype in a *lin-15A* background (Table 3A). We isolated a *mys-1* cDNA using RT-PCR and, by comparison to the genomic locus, determined a gene structure for *mys-1* (Figure 2A). The protein predicted by this cDNA is highly similar to the human Tip60 and the yeast Esa1p MYST family acetyltransferases (Figure 2B). MYS-1 is 72% identical to Tip60 and 62% identical to Esa1p in the acetyltransferase catalytic domain that defines MYST family proteins. In addition, all three contain an amino-terminal chromodomain, which is found in a small subset of MYST family acetyltransferases.

---

use of alternative splice acceptors would create small differences in the *trr-1* coding sequence: alternative splicings of the fourth (ag/TTTCAGAC versus agtttcag/AC), fifth (ag/AATCTTCAGTC versus agaatcttcag/TC), eleventh (ag/AACTTTAAGAT versus agaactttaag/AT), and twelfth introns (ag/TTGCAGAA versus agttgcag/AA) would result in differences of two or three amino acids.

(B) A schematic of the TRR-1 protein. All six *trr-1* mutations are predicted to prematurely truncate the TRR-1 protein. The positions and natures of these nonsense mutations are indicated above. TRR-1 is similar to mammalian TRRAP and yeast Tra1p throughout the lengths of the proteins. The degree of similarity is especially high in the FAT (FRAP, ATM, TRRAP-like) and ATM/PI-3 kinase-like domains, which are indicated with solid and hatched boxes, respectively.

(C–E) TRR-1 is expressed throughout development and is localized to nuclei. (C), a 4-cell stage embryo. (D), an L2 larva indicating TRR-1 expression in P4.p, P5.p, and P6.p (arrowheads). (E), a germline oocyte nucleus in an adult hermaphrodite. In (C) and (D), anterior is to the left and dorsal is up. To more clearly depict the weak expression of TRR-1 in somatic postembryonic cells in (D), we improved the signal-to-noise ratio of our initially captured image by adjusting pixel threshold values and applying a Gaussian filter using Adobe Photoshop 5.5. Scale bars, 5 μm.

(F–H) 4,6-Diamidino-2-phenylindole (DAPI) staining of the same samples shown in (C)–(E). In (E), P4.p, P5.p, and P6.p were identified by their positions and large, DAPI-negative nucleoli. In (F), the anterior-most cell, AB.a, and the dorsal-most cell, AB.p, have condensed mitotic chromosomes, which by comparison with (C) are not sites of concentrated TRR-1 localization. The discrete foci of DAPI staining in the oocyte nucleus shown in (H) indicate condensed meiotic chromosomes, and a comparison with (E) indicates localization of TRR-1 to these chromosomes. Scale bars, 5 μm.

Table 2. *trr-1* Epistasis with *let-23* RTK, *let-60* Ras, and *lin-3* EGF

Genotype	Average # P(3–8).p Vulval Fates ± SE	% Animals with >3 Vulval Fates	n
wild-type	3.00 ± 0	0	31
lin-15A(n767)	3.00 ± 0	0	24
lin-15B(n744)	3.00 ± 0	0	20
trr-1(RNAi)	3.09 ± 0.05	13	32
trr-1(n3712)	3.10 ± 0.03	13	89
trr-1(RNAi); lin-15A(n767)	5.60 ± 0.08	100	44
trr-1(n3712); lin-15B(n744)	3.38 ± 0.07	50	38
let-23(sy97); lin-15A(n767)	0 ± 0	0	21
let-23(sy97) trr-1(RNAi); lin-15A(n767)	0.21 ± 0.08	0	34
let-23(sy97); lin-15B(n744)	0.23 ± 0.08	0	26
let-23(sy97) trr-1(n3712); lin-15B(n744)	0.51 ± 0.10	0	38
let-60(n1876); lin-15A(n767)	0.02 ± 0.02	0	21
trr-1(RNAi); let-60(n1876); lin-15A(n767)	0.04 ± 0.04	0	22
let-60(n1876); lin-15B(n744)	0 ± 0	0	26
trr-1(n3712); let-60(n1876); lin-15B(n744)	0.34 ± 0.18	0	16
lin-3(n378); lin-15A(n767)	0.30 ± 0.07	0	40
trr-1(RNAi); lin-3(n378); lin-15A(n767)	4.35 ± 0.20	85	20
lin-3(n378); lin-15B(n744)	2.04 ± 0.16	0	27
trr-1(n3712); lin-3(n378); lin-15B(n744)	1.91 ± 0.21	9.1	33

let-23(sy97) homozygous mutants were recognized as Unc non-Gfp progeny of *let-23(sy97) unc-4(e120)/mIn1[dpy-10(e128) mIs14]* heterozygous parents, and *let-60(n1876)* homozygous mutants were recognized as Unc progeny of *let-60(n1876) unc-22(s7)/nT1; +/nT1* heterozygous parents. The combination of *trr-1(RNAi)* with the *trr-1(n3712)* mutation causes embryonic lethality (see Supplemental Data) and could not be used to approximate a null condition for *trr-1* in these tests. Because of its strong effect on gene activity, *trr-1(RNAi)* alone was used for epistasis tests in a *lin-15A* background. However, *trr-1(RNAi); lin-15B* mutants die early in development (see Supplemental Data), necessitating the use of *trr-1(n3712)* in epistasis tests with *lin-15B*.

mys-1 is located in the same genetic interval to which we had mapped the synMuv mutation *n3681*, which was isolated in the genetic screen that yielded our *trr-1* mutations (C.J.C., F. Stegmeier, M. Harrison, and H.R.H., unpublished data). *n3681* mutants are viable as homozygotes, although they have a reduced brood size compared to that of the wild-type (data not shown). Determination of the DNA sequence of *mys-1* in *n3681* mutants revealed a missense mutation predicted to change a conserved glycine residue in the acetyltransferase catalytic domain to an arginine (Figures 2A and 2B). As an indication that the extra vulval cell fates in *n3681; lin-15A(n767)* mutants were caused by the *mys-1* mutation, we found that a *mys-1* genomic clone restored the number of vulval cell fates in these animals to a wild-type level (Table 3A). *mys-1(n3681)* showed genetic interactions similar to those of *trr-1* mutations: *mys-1(n3681)* synthetically interacted with mutations in multiple class A synMuv genes (i.e., *lin-15A* and *lin-38*), *mys-1(n3681); synmuvA* mutants were synthetically defective in P3.p, P4.p, and P8.p cell-fate specification, and *mys-1(n3681); synmuvB* mutants showed synthetic P8.p ectopic vulval cell fates (Tables 3A and 3B).

We obtained a deletion mutation affecting the *mys-1* gene. This mutation, *n4075*, removes 1010 base pairs from the *mys-1* locus and is predicted to produce a protein that contains the first 35 amino acids of MYS-1 followed by 52 unrelated amino acids prior to termination (Figures 2A and 2B). The predicted full-length MYS-1 protein is 458 amino acids long, and the *n4075* deletion is expected to remove the conserved chromodomain and acetyltransferase catalytic domain. *mys-1(n4075)* mutants exhibited the same spectrum of abnormalities, namely slow growth, sterility, and weak defects in P8.p fate specification, as did our *trr-1* single

mutants. As with *mys-1(n3681)*, *mys-1(n4075)* synthetically interacted with both class A and class B synMuv mutations (Tables 3A and 3B).

Inactivation of a Homolog of the Tip60/NuA4 Complex Component Enhancer of Polycomb Causes Vulval Defects Like Those of *trr-1* and *mys-1* Mutants

The TIP60 and NuA4 complexes contain other proteins in addition to TRRAP/Tra1p and MYST family acetyltransferases (Galarneau et al., 2000; Ikura et al., 2000; Loewith et al., 2000). We inactivated *C. elegans* genes encoding homologs of these proteins and identified *epc-1* as a negative regulator of vulval induction (Table 3). *epc-1* encodes a homolog of the *Drosophila* Enhancer of Polycomb [E(Pc)] protein and similarly named mammalian and yeast proteins. Injection of *epc-1* dsRNA into wild-type hermaphrodites caused fully penetrant embryonic lethality. To study the effects of *epc-1* inactivation during postembryonic development, we injected *epc-1* dsRNA into *rde-1* RNAi-deficient hermaphrodites and mated these animals with RNAi-competent males, a procedure referred to as "zygotic RNAi" (Herman, 2001). The lack of RNAi efficacy in the maternal germline allows progeny of such matings to inherit an active maternal complement of gene activity. Since these *rde-1/+* progeny are RNAi competent, zygotic gene activity is subject to the effects of RNAi. For some genes that act during multiple stages of development, zygotic RNAi has been shown to result in sufficient gene activity for embryonic functions but inadequate gene activity for postembryonic functions (Herman, 2001). *epc-1(RNAi)* performed in this manner did not affect vulval development in wild-type animals but produced

Table 3. *mys-1* and *epc-1* Mutants Are Defective in Vulval Cell-Fate Specification

A. Inactivation of TRRAP Complex Homologs in *synmuvA* Mutant Backgrounds

Genotype	Homolog(s) of Inactivated Gene	Average # P(3–8).p Vulval Fates ± SE	% Animals with >3 Vulval Fates	n
wild-type	-	3.00 ± 0	0	31
lin-15A(n767)	-	3.00 ± 0	0	24
lin-38(n751)	-	3.00 ± 0	0	27
Y47G6A.6(RNAi); lin-15A(n767)	Gcn5 family HATs	3.00 ± 0	0	62
mys-1(RNAi); lin-15A(n767)	MYST family HATs	4.29 ± 0.23	71	24
mys-1(n3681); lin-15A(n767)	MYST family HATs	5.04 ± 0.14	100	26
mys-1(n3681); lin-15A(n767); Ex[mys-1]	MYST family HATs	3.02 ± 0.02	4.3	23
lin-38(n751); mys-1(n3681)	MYST family HATs	4.40 ± 0.13	91	45
mys-1(n4075); lin-15A(n767)	MYST family HATs	3.76 ± 0.14	76	25
mys-1(n4075); lin-38(n751)	MYST family HATs	3.89 ± 0.18	72	22
C34B7.4(RNAi); lin-15A(n767)	MYST family HATs	3.00 ± 0	0	29
K03D10.3(RNAi); lin-15A(n767)	MYST family HATs	3.00 ± 0	0	24
R07B5.8(RNAi); lin-15A(n767)	MYST family HATs	0.14 ± 0.06	0	26
epc-1(RNAi); lin-15A(n767)	*H.s.* Tip60 and *S.c.* NuA4 component E(Pc) family proteins	3.32 ± 0.10	36	33
epc-1(n4076); lin-15A(n767)	*H.s.* Tip60 and *S.c.* NuA4 component E(Pc) family proteins	ND	-	-
lin-38(n751); epc-1(RNAi)	*H.s.* Tip60 and *S.c.* NuA4 component E(Pc) family proteins	3.29 ± 0.02	31	65
ssl-1(n4077); lin-15A(n767)	*H.s.* p400	3.00 ± 0	0	36
T22D1.1(RNAi); lin-15A(n767)	*H.s.* Tip60 component TAP54a/ TIP49a/RUVBL1	3.00 ± 0	0	31
C27H6.2(RNAi); lin-15A(n767)	*H.s.* Tip60 component TAP54b/ TIP49b/RUVBL2	3.00 ± 0	0	22
Y37D8A.9(RNAi); lin-15A(n767)	*S.c.* NuA4 component Eaf3p	3.00 ± 0	0	24
Y51H1A.4(RNAi); lin-15A(n767)	*S.c.* NuA4 component Yng2p	3.00 ± 0	0	20
M04B2.3(RNAi); lin-15A(n767)	*S.c.* Tra1p interacting protein Yaf9p	3.00 ± 0	0	29

B. *mys-1*, *epc-1*, and *ssl-1* Single Mutants and Interactions with *lin-15B*

Genotype	% Animals with P8.p Vulval Fate	n
wild-type	0	31
lin-15B(n744)	0	20
mys-1(n3681)	8.3	36
mys-1(n4075)	15	20
epc-1(RNAi)	0	65
epc-1(n4076)	ND	-
ssl-1(n4077)	0	37
mys-1(n3681); lin-15B(n744)	46	37
mys-1(n4075); lin-15B(n744)	77	31
epc-1(RNAi); lin-15B(n744)	4.2	48
ssl-1(n4077); lin-15B(n744)	72	25

mys-1(n4075) homozygous mutants were recognized as the non-Unc progeny of +/*nT1(n754)*; *mys-1(n4075)/nT1(n754)* heterozygous parents, and *trr-1* homozygous mutants were recognized as the non-Gfp progeny of *trr-1(n3712)/mln1[dpy-10(e128) mls14]* heterozygous parents. Since injection of *epc-1*, *ssl-1*, *T22D1.1* and *C27H6.2* dsRNAs into wild-type hermaphrodites caused highly penetrant embryonic lethality, we performed "zygotic RNAi" as described in the text; consequently, the complete genotypes of the *epc-1(RNAi)*, *ssl-1(RNAi)*, *T22D1.1(RNAi)*, and *C27H6.2(RNAi)* strains included *rde-1(ne219)/+*. In addition to the TRRAP complex proteins described in Results, TAP54a/TIP49a/RUVBL1 and TAP54b/TIP49b/RUVBL2 are components of the human Tip60 complex (Ikura et al., 2000); Eaf3p (Eisen et al., 2001) and Yng2p (Loewith et al., 2000) are components of the yeast NuA4 complex; and Yaf9p coimmunoprecipitates with Tra1p in yeast extracts (Gavin et al., 2002). ND, not determined (see text); *H.s.*, *Homo sapiens*; *S.c.*, *Saccharomyces cerevisiae*.

a Muv phenotype in *lin-15A* and *lin-38* mutant backgrounds (Table 3A). A low percentage of P8.p vulval cell fates was observed in a *lin-15B* background (Table 3B). We obtained a deletion allele, *n4076*, that removes 886 bases from the *epc-1* locus, including the third and fourth *epc-1* exons (Figure 2C). If the second exon were spliced to the fifth exon, a 137 amino acid protein would be produced that contains the first 109 amino acids of the 795 amino acid predicted EPC-1 protein. *epc-1(n4076)* homozygotes typically hatched with proper morphology and a normal number of cells, but died shortly thereafter. Because of this lethality, we were unable to measure vulval defects in *epc-1(n4076)* mutants.

ssl-1, a p400 SWI/SNF ATPase Homolog, Acts Redundantly with *lin-15B*

TRRAP is a component of the mammalian p400 complex, which contains the p400 SWI/SNF family protein and was identified based on its interaction with the adenovirus E1A oncoprotein (Fuchs et al., 2001). Although Tip60 was not present in the purified p400 complex, the Tip60 and p400 complexes share many of the same components and more recent analyses have indicated
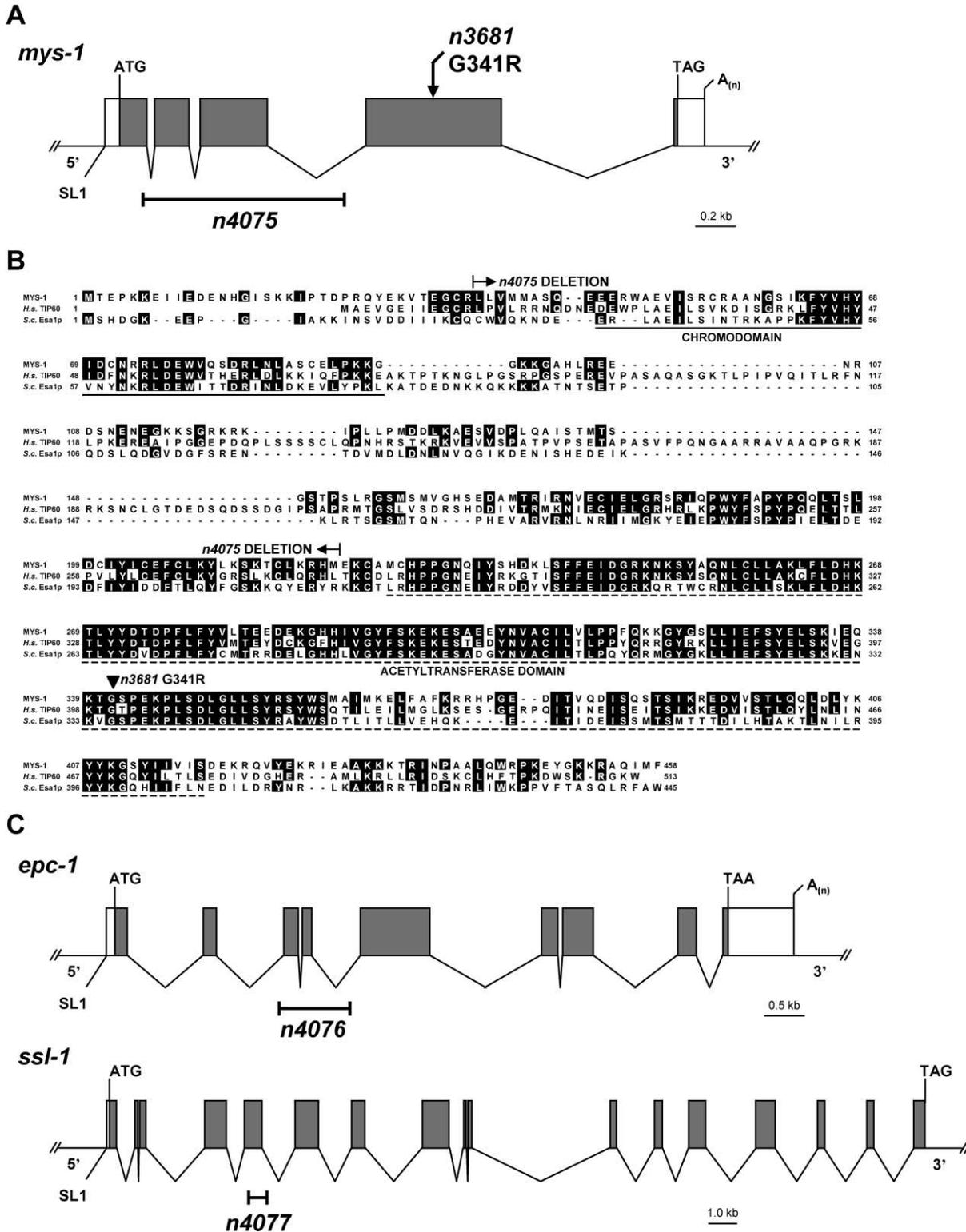
A

B

C

Figure 2. *mys-1*, *epc-1*, and *ssl-1* Gene Structures and Mutations

(A) The *mys-1* gene structure as derived from cDNA and genomic sequences. Shaded boxes indicate coding sequence and open boxes indicate 5′ and 3′ untranslated regions. Predicted translation initiation and termination codons and the poly(A) tail are shown. An arrow above indicates the position of the *mys-1(n3681)* mutation and a bracket below indicates the sequence deleted by *mys-1(n4075)*.

(B) Alignment of the MYS-1 protein with the human Tip60 (GenBank accession number NP006379) and yeast Esa1p (NP014887) histone acetyltransferases. Solid boxes indicate identities with MYS-1. An arrowhead indicates the *mys-1(n3681)* mutation, and brackets indicate the sequence removed by *mys-1(n4075)*. Animals containing the *mys-1(n4075)* deletion are expected to produce only the first 35 amino acids of

that p400 and Tip60 can copurify as part of a large p400/Tip60 multisubunit complex (Frank et al., 2003).

The *C. elegans* gene *ssl-1* (*ssl*, SWI/SNF-like) encodes a homolog of the p400 protein. Injection of *ssl-1* dsRNA into wild-type hermaphrodites caused fully penetrant embryonic lethality like that observed with *epc-1(RNAi)*. zygotic RNAi of *ssl-1*, performed as described above, did not cause defects in vulval development in either class A or class B synMuv backgrounds (data not shown). We isolated a deletion mutation, *n4077*, that removes a portion of the fifth *ssl-1* exon (Figure 2C). *ssl-1(n4077)* is predicted to encode a truncated protein containing the first 540 amino acids of the 2395 amino acid SSL-1 protein and two unrelated amino acids. *ssl-1(n4077)* homozygotes were partially sterile and produced a few inviable embryos (data not shown) but were not defective in vulval development (Table 3). *ssl-1(n4077); lin-15A(n767)* mutants were likewise not defective in vulval development. However, *ssl-1(n4077); lin-15B(n744)* mutants often expressed an ectopic vulval cell fate in P8.p. *ssl-1(n4077)* likely causes a stronger reduction in gene activity than does *ssl-1* zygotic RNAi, and this stronger reduction unmasks a redundancy between *ssl-1* and *lin-15B*.

trr-1; mys-1, trr-1; epc-1, and *trr-1; ssl-1* Double Mutants Do Not Show Synthetic Defects in Vulval Development

Whereas synthetic defects in double mutants suggest functional redundancy, the lack of synthetic defects in double mutants can indicate that two genes act in the same genetic pathway. Based on the similar phenotype and genetic interactions of *trr-1*, *mys-1*, and *epc-1* mutants and on the copurification of the proteins encoded by their mammalian and yeast counterparts, we hypothesized that *trr-1*, *mys-1*, and *epc-1* act together to regulate vulval development (because its genetic interactions slightly differ from those of *trr-1*, *mys-1*, and *epc-1*, *ssl-1* will be discussed separately below). We constructed double mutants to determine if *mys-1* and *epc-1* function redundantly with *trr-1*. We measured the numbers of vulval cell fates in *trr-1(n3712); mys-1(n3681)*, *trr-1(n3712); mys-1(n4075)*, and *trr-1(n3712); epc-1(RNAi)* mutants and found that the extent of vulval development observed in these double mutants was similar to that observed in single mutant animals (Table 4). These results suggest that *mys-1* and *epc-1* act in the same genetic pathway as *trr-1*, which by analogy to the class A and class B *lin-35* Rb synMuv pathways we have named the class C synMuv pathway.

In general, animals carrying mutations in two genes of the same synMuv class do not show a synthetic phenotype. *trr-1; ssl-1* double mutants (Table 4) and, as described above, *ssl-1; lin-15A* mutants were not synthetically defective in the specification of P(3–8).p cell fates. It is possible that *ssl-1* has both class C and class

A synMuv activities. However, additional considerations suggest that *ssl-1* has properties more like those of a class C gene. For instance, *ssl-1; synmuvB* mutants have a defect limited to P8.p, whereas *synmuvA; synmuvB* mutants typically show ectopic vulval cell fates expressed by P3.p, P4.p, and P8.p. In addition, *ssl-1* mutants are sterile, and sterility has not been observed for any class A synMuv mutant (Thomas et al., 2003). These considerations, along with the copurification of the mammalian SSL-1 and MYS-1 counterparts p400 and Tip60, suggest that *ssl-1* is an atypical class C gene, one that acts redundantly with class B but not class A synMuv genes. It is possible that *ssl-1* defines a subtype of class C genes that distinguishes the subset of processes mediated by class C activity redundant with class B activity from the subset redundant with class A activity.

Discussion

trr-1, *mys-1*, *epc-1*, and *ssl-1* Act Redundantly with the *lin-35* Rb Pathway to Antagonize *let-60* Ras Signaling

trr-1, *mys-1*, *epc-1*, and *ssl-1* act in the determination of vulval cell fates, since they help distinguish P3.p, P4.p, and P8.p from P(5–7).p. In many cases, pathways that control cell-fate determination in invertebrates have been found to regulate similar processes in mammals. Pathways that regulate vulval cell-fate specification in *C. elegans* provide clear examples: a conserved *let-60* Ras pathway induces vulval cell fates, and this pathway is antagonized by an at least partially conserved class B *lin-35* Rb pathway (Saito and van den Heuvel, 2002). We have found that *trr-1*, *mys-1*, *epc-1*, and *ssl-1* act in parallel to *lin-35* Rb and other synMuv genes to negatively regulate *let-60* Ras signaling. We suggest that the mammalian counterparts of *trr-1*, *mys-1*, *epc-1*, and *ssl-1* may similarly act in parallel to Rb and antagonize Ras in the control of cell-fate determination and cell division and that dysregulation of these mammalian counterparts may contribute to oncogenesis. It is interesting to note that the p400 complex and Rb-containing complexes are targeted by the adenovirus E1A oncoprotein (Whyte et al., 1988; Fuchs et al., 2001). Our finding that *ssl-1* acts redundantly with a *lin-35* Rb pathway gene suggests that E1A may act in mammals by perturbing the activities of functionally redundant p400- and Rb-containing complexes.

TRR-1, MYS-1 and EPC-1 May Be Components of a Histone Acetyltransferase Complex

The vulval phenotypes and genetic interactions of *trr-1*, *mys-1*, and *epc-1* mutants are strikingly similar. Given the biochemical copurification of their mammalian and yeast counterparts, these data strongly suggest that TRR-1, MYS-1, and EPC-1 proteins function as part of

---

the wild-type MYS-1 protein and additional frameshifted amino acids prior to truncation. The chromodomain and acetyltransferase domains are underlined with solid and dashed lines, respectively.

(C) *epc-1* (top) and *ssl-1* (bottom) gene structures as derived from cDNA and genomic sequences. Shaded boxes indicate coding sequence and open boxes indicate 5′ and 3′ untranslated regions. We were unable to identify a 3′ untranslated region for *ssl-1*. Predicted translation initiation and termination codons and the *epc-1* poly(A) tail is shown. Brackets indicate the sequences deleted by *epc-1(n4076)* and *ssl-1(n4077)*.

Table 4. *mys-1*, *epc-1*, and *ssl-1* Do Not Synthetically Interact with *trr-1*

Genotype	Average # P(3–8).p Vulval Fates ± SE	% Animals with >3 Vulval Fates	n
wild-type	3.00 ± 0	0	31
trr-1(n3712)	3.10 ± 0.03	13	89
mys-1(n3681)	3.06 ± 0.03	8.3	36
mys-1(n4075)	3.15 ± 0.08	15	20
epc-1(RNAi)	3.00 ± 0	0	65
ssl-1(n4077)	3.00 ± 0	0	37
trr-1(n3712); mys-1(n3681)	3.15 ± 0.06	22	27
trr-1(n3712); mys-1(n4075)	3.05 ± 0.05	9.1	11
trr-1(n3712); epc-1(RNAi)	3.08 ± 0.04	10	30
trr-1(n3712); ssl-1(n4077)	3.08 ± 0.05	12	25

mys-1(n4075) homozygous mutants were recognized as the non-Unc progeny of +/*nT1(n754)*; *mys-1(n4075)/nT1(n754)* heterozygous parents, and *trr-1* homozygous mutants were recognized as the non-Gfp progeny of *trr-1(n3712)/mln1[dpy-10(e128) mls14]* heterozygous parents. "zygotic RNAi" of *epc-1* was performed as described in the text; consequently, the complete genotypes of *epc-1(RNAi)* mutants include *rde-1(ne219)/+*.

a multisubunit complex that acetylates histones and possibly other proteins. Many histone acetyltransferase complexes have been biochemically purified, and these complexes are distinguished by their subunit compositions and substrate specificities. Although certain subunits such as mammalian TRRAP and yeast Tra1p are found in many different complexes, only the mammalian Tip60 and yeast NuA4 complexes are known to contain homologs of all three of the proteins described in this study. It is possible that a TRR-1/MYS-1/EPC-1 complex is a *C. elegans* counterpart of one or both of these complexes. To further address this possibility, we inactivated genes encoding *C. elegans* homologs of the Tip60 and NuA4 complex proteins TAP54α/TIP49a/RUVBL1, TAP54β/TIP49b/RUVBL2, Eaf3p, Yng2p, and Yaf9p (Ikura et al., 2000; Loewith et al., 2000; Eisen et al., 2001; Gavin et al., 2002). We did not observe a synthetic interaction with a class A mutation for any of the homologs targeted. These *C. elegans* homologs may therefore not be components of the putative TRR-1/MYS-1/EPC-1 complex. However, it remains possible that inactivation of these homologs will reveal a redundancy with class B synMuv proteins, suggesting action, like SSL-1, in a subset of the processes regulated by the putative TRR-1/MYS-1/EPC-1 complex.

Histone acetyltransferases have been characterized as transcriptional coactivators (Roth et al., 2001), and TRRAP and its yeast homolog Tra1p are proposed to bridge interactions between activation domains of DNA binding transcription factors and histone acetyltransferases (Brown et al., 2001). Therefore, a putative TRR-1/MYS-1/EPC-1 complex may function in transcriptional activation. If so, we would expect it to activate genes that negatively regulate vulval development.

TRRAP has been proposed to interact with DP/E2F heteromeric transcription factors and recruit the histone acetyltransferase GCN5 to activate expression of DP/E2F target genes (McMahon et al., 2000; Lang et al., 2001). We tested this hypothesis by constructing *dpl-1 trr-1* double mutants and measuring whether or not these mutants showed synthetic phenotypes. We found that *dpl-1* and *trr-1* interacted to produce synthetic vulval defects and synthetic lethality. These observations suggest that *trr-1* does not act through *dpl-1*, although we cannot exclude the possibility that *trr-1* acts through

both *dpl-1* and an as yet undefined pathway acting in parallel to *dpl-1*.

While most data support the link between acetylation and activation, a few observations suggest that at least some histone acetylation may be important for transcriptional silencing. For example, loss-of-function mutations that affect the MYST family acetyltransferases Sas2p and Sas3p cause defects in the silencing of mating type loci and telomeres in yeast (Reifsnyder et al., 1996; Ehrenhofer-Murray et al., 1997). Sas2p is proposed to acetylate newly deposited nucleosomes, and the modified acetyllysine residues it creates are thought to be important for establishing silencing following DNA replication (Meijsing and Ehrenhofer-Murray, 2001; Osada et al., 2001). Just as a MYST family histone acetyltransferase is linked to silencing, there may be a role in *Drosophila* for E(Pc) in transcriptional repression. *E(Pc)* mutations synergize with polycomb group mutations to strongly derepress homeobox genes and act alone as suppressors of variegation to derepress genes that are juxtaposed to heterochromatin (Sato et al., 1983; Sinclair et al., 1998).

These observations allow us to consider the possibility that MYS-1, in association with TRR-1 and EPC-1, may normally downregulate transcription. According to this hypothesis, we would expect a putative TRR-1/MYS-1/EPC-1 complex to repress genes that are required for vulval cell fates, possibly the same genes that are repressed by LIN-35 Rb and other class B synMuv proteins. Because we do not know the relevant targets of either TRR-1/MYS-1/EPC-1 or the class B synMuv proteins and because we have been unable to detect globally reduced histone acetylation in *mys-1* mutants using commercially available antibodies that specifically recognize acetylated histone isoforms (our unpublished data), we have no basis for distinguishing whether the putative TRR-1/MYS-1/EPC-1 complex acts in transcriptional activation or repression.

Chromatin Remodeling and Modification Limits Inductive Signaling in Vulval Development

Our findings have led us to consider the effects of chromatin remodeling and modification on developmental processes. The phenotypes of *trr-1*, *mys-1*, *epc-1*, and *ssl-1* mutants and the localization of the TRR-1 protein

A) In wild-type animals Ras pathway activity in P(3-8).p cells must exceed a threshold for these cells to adopt vulval fates
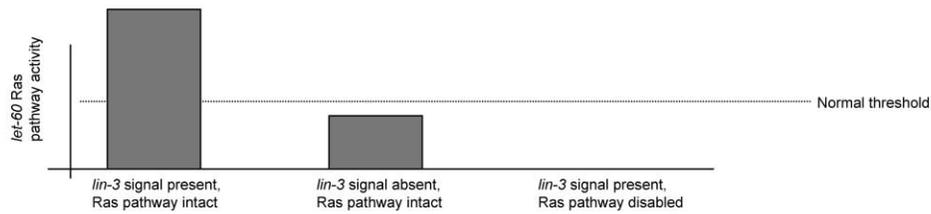
B) Model 1: synMuv genes modulate the threshold but not absolute levels of Ras pathway activity
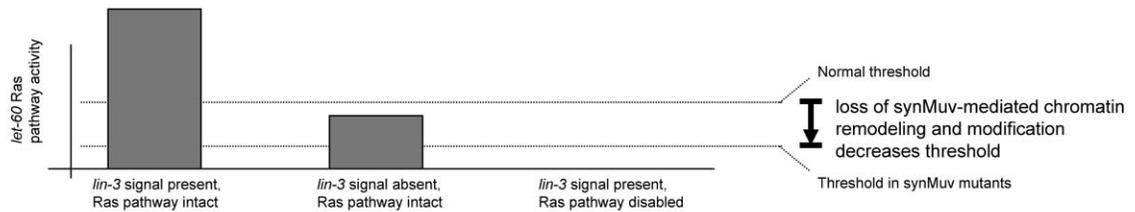
C) Model 2: synMuv genes modulate absolute levels of Ras pathway activity and leave the threshold unchanged
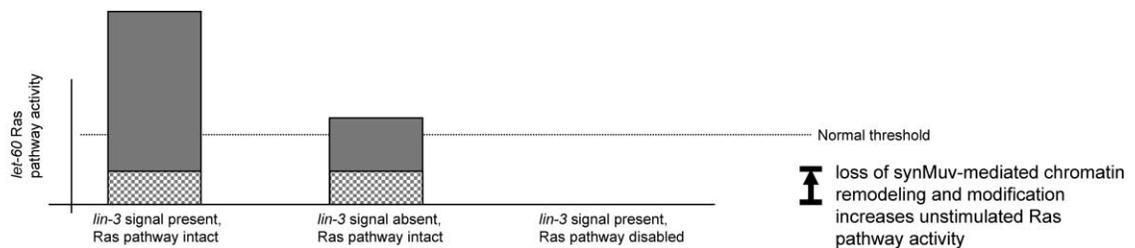

Figure 3. Models for How the synMuv Genes May Limit the Extent of Inductive Signaling

(A) *let-60* Ras pathway activity is required for vulval cell fates, and we propose that the level of activity must exceed a predetermined threshold for a cell to adopt a vulval fate. When the LIN-3 EGF-like signal is present and Ras pathway intact (left), as with P(5–7).p of wild-type animals, the level of activity exceeds this threshold. However, when the LIN-3 signal is absent and Ras pathway intact (middle), as with P3.p, P4.p, and P8.p of wild-type animals or P(3–8).p of *lin-3* mutants, this threshold is not reached by basal, unstimulated Ras pathway activity. Ras pathway activity in P(3–8).p is abrogated by *let-23* RTK, *let-60* Ras, and other mutations that disable Ras pathway components (right).

(B) Model 1: The synMuv genes may increase the threshold of Ras pathway activity that is required for vulval cell fates. In P3.p, P4.p, and P8.p of *synmuv* mutants or in P(3–8).p of *lin-3; synmuv* mutants (middle), the threshold of activity required for vulval cell fates is lowered such that a basal, unstimulated level of Ras pathway activity is sufficient for these cells to adopt vulval cell fates. However, mutations in core Ras pathway components such as *let-60* Ras (right) diminish Ras pathway activity to a level that cannot overcome the lower threshold resulting from synMuv mutations.

(C) Model 2: The synMuv genes may decrease absolute levels of Ras pathway activity and leave the threshold of activity required for vulval cell fates unaffected. In P3.p, P4.p, and P8.p of *synmuv* mutants or in P(3–8).p of *lin-3; synmuv* mutants (middle), Ras pathway activity is increased to a level that is sufficient for these to adopt vulval cell fates. synMuv mutations have no effect in mutants lacking core Ras pathway function (right).

are consistent with the hypothesis that the class C synMuv genes act within P(3–8).p. Some class B synMuv genes are also proposed to act in P(3–8).p (Lu and Horvitz, 1998; Thomas and Horvitz, 1999; Ceol and Horvitz, 2001), suggesting that multiple chromatin remodeling and modification activities act in the same cells to regulate cell-fate specification. How might these activities together specify P(3–8).p fates?

In general, the class C and other synMuv genes prevent cells that do not receive inductive signal from adopting vulval fates (Figure 3A). At the time of vulval induction, the LIN-3 EGF ligand is produced by the gonadal anchor cell and stimulates Ras pathway signaling in the neighboring cells P(5–7).p. The high levels of Ras pathway activity in P(5–7).p exceed a predetermined threshold that is required for the adoption of vulval cell fates. Because of their distance from the anchor cell, P3.p, P4.p, and P8.p receive little to no LIN-3 signal, and the unstimulated level of Ras pathway activity in these cells is insufficient to induce vulval fates.

In one model, the synMuv genes may establish the high threshold that distinguishes the responses of cells that receive from those of cells that do not receive inductive signal (Figure 3B). In synMuv mutants, this threshold is reduced in P(3–8).p to a level that can be exceeded even by unstimulated, that is, LIN-3-independent, Ras pathway activity.

Alternatively, instead of increasing the threshold for a response to Ras pathway activity, the synMuv genes may decrease the absolute level of Ras pathway activity

in P(3–8).p (Figure 3C). In this model, synMuv mutations boost unstimulated Ras pathway activity, such as that in P3.p, P4.p, and P8.p of wild-type animals or in P(3–8).p of *lin-3* mutants, to a level that exceeds an unchanged threshold for vulval fates. It should be noted, however, that we have not detected an increased level of Ras pathway activity in synMuv mutants, as measured by Western blots of activated diphosphorylated *C. elegans* MPK-1 MAP kinase (data not shown).

Ras signaling during vulval development acts through the LIN-1 ETS and LIN-31 winged helix transcription factors (Miller et al., 1993; Beitel et al., 1995; Tan et al., 1998). It is unclear whether chromatin remodeling and modification by the synMuv genes impacts transcription by LIN-1 and LIN-31 or whether the synMuv and Ras pathways converge in a less direct manner. Whatever the point of convergence, the synMuv genes likely act to limit the extent of Ras-mediated vulval induction. We suggest that chromatin remodeling and modification may be used as a general mechanism to limit inductive signaling in developing organisms.

Experimental Procedures

Strains and Genetics

Strains were cultured as described by Brenner (1974) and maintained at 20°C unless otherwise specified. Bristol N2 was used as the wild-type strain. The following mutations were used: LGI: *lin-35(n745)*; LGII: *dpy-10(e128)*, *let-23(sy97)*, *dpl-1(n2994, n3316)* (Ceol and Horvitz, 2001), *unc-4(e120)*, *trr-1(n3630, n3637, n3704, n3708, n3709, n3712)* (this study), *mex-1(it9)*, *lin-38(n751)*; LGIII: *lon-1(e185)*, *sup-5(e1464)*, *lin-36(n766, n3096)* (Thomas and Horvitz, 1999), *lin-37(n758)*, *epc-1(n4076)* (this study), *ssl-1(n4077)* (this study), *unc-25(e156)*; LGIV: *lin-3(n378)*, *let-60(n1876)* (Beitel et al., 1990), *unc-22(s7)*; LGV: *unc-46(e177)*, *mys-1(n3681, n4075)* (this study), *dpy-11(e224)*, *rde-1(ne219)* (Tabara et al., 1999); and LGX: *lin-15B(n744)*, *lin-15A(n767, n433)* (Ferguson and Horvitz, 1989). The deficiency *mnDf90*, translocation *nT1(n754)* (IV;V), translocation *eT1* (IV;V), and chromosomal inversion *mIn1[dpy-10(e128) mIs14]* were also used. *mIs14*, an integrated transgene linked to the chromosomal inversion *mIn1*, consists of a combination of GFP-expressing transgenes that allows animals carrying *mIs14* to be identified beginning at the 4-cell stage of embryogenesis (Edgley and Riddle, 2001). Unless otherwise noted, the mutations and chromosomal aberrations are described by Riddle et al. (1997).

Assay for P(3–8).p Vulval Cell Fates

Cell fates were scored in L4 hermaphrodites using Nomarski microscopy by counting the number of descendants that had been produced by individual P(3–8).p cells. Scores of 1, 0.5, and 0, were assigned to cells that fully, partially, or did not adopt vulval cell fates, respectively. P(3–8).p cells that partially adopt a vulval cell fate have one daughter that divided to produce two to four descendants and another daughter that remained undivided.

Cloning of *trr-1* and *mys-1*

Using standard deficiency (Sigurdson et al., 1984) and three-point mapping (Brenner, 1974) techniques, we placed the *n3712* mutation in an interval on LGII between the right endpoint of the deficiency *mnDf90* and the *mex-1* gene (data not shown). To clone the gene affected by *n3712*, we performed transformation rescue as described by Mello et al. (1991), using the pRF4 plasmid (80 ng/μl) as a coinjection marker. We rescued the *n3712* Muv and sterile phenotypes by injecting the *trr-1*-containing cosmid C47D12 (10 ng/μl) into *n3712/ mIn1[dpy-10(e128) mIs14]; lin-15A(n767)* mutants and isolating Rol non-Gfp transgenic lines. We performed RNA-mediated interference (RNAi) of *trr-1* and determined that it caused the same abnormalities as *n3712* (see Results). We mapped *n3681* between *unc-46* and *dpy-11* on LGV. Because of the relationship between the mammalian and yeast *mys-1* and *trr-1* counterparts,

we injected a 9.9 kb XhoI *mys-1* genomic clone derived from the cosmid VC5 (50 ng/μl) and the *sur-5::gfp*-expressing construct pTG96 (50 ng/μl; kindly provided by M. Han) as a coinjection marker into and observed rescue of the Muv phenotype of *n3681; lin-15A(n767)* mutants.

Isolation of Deletion Alleles

Genomic DNA pools from mutagenized worms were screened for deletions as described by Ceol and Horvitz (2001). Deletion mutant animals were isolated from frozen stocks and were backcrossed four times to the wild-type prior to use. *mys-1(n4075)* removes nucleotides +106 to +1115, *epc-1(n4076)* nucleotides +2014 to +2899, and *ssl-1(n4077)* nucleotides +5075 to +5757 of genomic DNA relative to their respective predicted translational start sites (predicted translational start sites and surrounding genomic DNA are found in GenBank files AF106581 [*mys-1*] and AL132904 [*epc-1* and *ssl-1*]).

RNAi Analyses

Templates for in vitro transcription reactions were made by PCR amplification of either cDNAs and their flanking T3 and T7 promoter sequences or coding exons from genomic DNA using T3- and T7-tagged oligonucleotides. In vitro transcribed RNA was denatured for 10 min and annealed prior to injection.

cDNA Isolation

We used RT-PCR (Titan one-tube RT-PCR, Roche Diagnostics) and total RNA from wild-type animals as a template to obtain *trr-1*, *mys-1*, and *ssl-1* cDNA clones. Existing cDNAs were obtained from the *C. elegans* EST project (kindly provided by Y. Kohara and coworkers) to determine gene structures of *epc-1*, the *ssl-1* 5′ end, and the *trr-1* 3′ end. We used 5′ RACE (5′ RACE System v2.0, GIBCO) to determine the 5′ ends and SL1 *trans*-spliced leader sequences of *trr-1*, *mys-1*, and *epc-1* transcripts.

Determination of Mutant Allele Sequences

We used PCR-amplified regions of genomic DNA as templates in determining mutant allele sequences. For each allele investigated, we determined the sequences of both strands of all exons and splice junctions of the gene in question. All mutations were confirmed by determining the sequences of independently derived PCR products. Sequences were determined using an automated ABI 373 DNA sequencer (Applied Biosystems).

Antibody Staining

Antibodies recognizing TRR-1 were generated by injecting a glutathione S-transferase-tagged carboxy-terminal fragment of TRR-1, GST-TRR-1(3280-4064), into two rabbits. Anti-TRR-1 antibodies were affinity purified using a maltose binding protein-tagged carboxy-terminal TRR-1 fragment, MBP-TRR-1(3280-4064), as described (Koelle and Horvitz, 1996). Embryos, larvae, and adults were fixed according to Finney and Ruvkun (1990). Affinity-purified antibodies were used at a 1:100 dilution for whole-mount staining. FITC-conjugated goat anti-rabbit secondary antibody (Jackson Laboratories) was used for detection.

References

Allard, S., Utley, R.T., Savard, J., Clarke, A., Grant, P., Brandl, C.J., Pillus, L., Workman, J.L., and Cote, J. (1999). NuA4, an essential transcription adaptor/histone H4 acetyltransferase complex containing Esa1p and the ATM-related cofactor Tra1p. EMBO J. *18*, 5108–5119.

Becker, P.B., and Horz, W. (2002). ATP-dependent nucleosome remodeling. Annu. Rev. Biochem. *71*, 247–273.

Beitel, G.J., Clark, S.G., and Horvitz, H.R. (1990). *Caenorhabditis elegans ras* gene *let-60* acts as a switch in the pathway of vulval induction. Nature *348*, 503–509.

Beitel, G.J., Tuck, S., Greenwald, I., and Horvitz, H.R. (1995). The *Caenorhabditis elegans* gene *lin-1* encodes an ETS-domain protein and defines a branch of the vulval induction pathway. Genes Dev. *9*, 3149–3162.

Brenner, S. (1974). The genetics of *Caenorhabditis elegans*. Genetics *77*, 71–94.

Brown, C.E., Lechner, T., Howe, L., and Workman, J.L. (2000). The many HATs of transcription coactivators. Trends Biochem. Sci. *25*, 15–19.

Brown, C.E., Howe, L., Sousa, K., Alley, S.C., Carrozza, M.J., Tan, S., and Workman, J.L. (2001). Recruitment of HAT complexes by direct activator interactions with the ATM-related Tra1 subunit. Science *292*, 2333–2337.

Ceol, C.J., and Horvitz, H.R. (2001). *dpl-1* DP and *efl-1* E2F act with *lin-35* Rb to antagonize Ras signaling in *C. elegans* vulval development. Mol. Cell *7*, 461–473.

Edgley, M.L., and Riddle, D.L. (2001). LG II balancer chromosomes in *Caenorhabditis elegans*: *mT1*(II;III) and the *mln1* set of dominantly and recessively marked inversions. Mol. Genet. Genomics *266*, 385–395.

Ehrenhofer-Murray, A.E., Rivier, D.H., and Rine, J. (1997). The role of Sas2, an acetyltransferase homologue of *Saccharomyces cerevisiae*, in silencing and ORC function. Genetics *145*, 923–934.

Eisen, A., Utley, R.T., Nourani, A., Allard, S., Schmidt, P., Lane, W.S., Lucchesi, J.C., and Cote, J. (2001). The yeast NuA4 and *Drosophila* MSL complexes contain homologous subunits important for transcription regulation. J. Biol. Chem. *276*, 3484–3491.

Ferguson, E.L., and Horvitz, H.R. (1989). The multivulva phenotype of certain *Caenorhabditis elegans* mutants results from defects in two functionally redundant pathways. Genetics *123*, 109–121.

Finney, M., and Ruvkun, G. (1990). The *unc-86* gene product couples cell lineage and cell identity in *C. elegans*. Cell *63*, 895–905.

Frank, S.R., Parisi, T., Taubert, S., Fernandez, P., Fuchs, M., Chan, H.M., Livingston, D.M., and Amati, B. (2003). MYC recruits the TIP60 histone acetyltransferase complex to chromatin. EMBO Rep. *4*, 575–580.

Fuchs, M., Gerber, J., Drapkin, R., Sif, S., Ikura, T., Ogryzko, V., Lane, W.S., Nakatani, Y., and Livingston, D.M. (2001). The p400 complex is an essential E1A transformation target. Cell *106*, 297–307.

Galarneau, L., Nourani, A., Boudreault, A.A., Zhang, Y., Heliot, L., Allard, S., Savard, J., Lane, W.S., Stillman, D.J., and Cote, J. (2000). Multiple links between the NuA4 histone acetyltransferase complex and epigenetic control of transcription. Mol. Cell *5*, 927–937.

Gavin, A.C., Bosche, M., Krause, R., Grandi, P., Marzioch, M., Bauer, A., Schultz, J., Rick, J.M., Michon, A.M., Cruciat, C.M., et al. (2002). Functional organization of the yeast proteome by systematic analysis of protein complexes. Nature *415*, 141–147.

Han, M., and Sternberg, P.W. (1990). *let-60*, a gene that specifies cell fates during *C. elegans* vulval induction, encodes a ras protein. Cell *63*, 921–931.

Herman, M. (2001). *C. elegans* POP-1/TCF functions in a canonical Wnt pathway that controls cell migration and in a noncanonical Wnt pathway that controls cell polarity. Development *128*, 581–590.

Hill, R.J., and Sternberg, P.W. (1992). The gene *lin-3* encodes an inductive signal for vulval development in *C. elegans*. Nature *358*, 470–476.

Hunter, T. (1995). When is a lipid kinase not a lipid kinase? When it is a protein kinase. Cell *83*, 1–4.

Ikura, T., Ogryzko, V.V., Grigoriev, M., Groisman, R., Wang, J., Horikoshi, M., Scully, R., Qin, J., and Nakatani, Y. (2000). Involvement of the TIP60 histone acetylase complex in DNA repair and apoptosis. Cell *102*, 463–473.

Kimble, J. (1981). Alterations in cell lineage following laser ablation of cells in the somatic gonad of *Caenorhabditis elegans*. Dev. Biol. *87*, 286–300.

Koelle, M.R., and Horvitz, H.R. (1996). EGL-10 regulates G protein signaling in the *C. elegans* nervous system and shares a conserved domain with many mammalian proteins. Cell *84*, 115–125.

Lang, S.E., McMahon, S.B., Cole, M.D., and Hearing, P. (2001). E2F transcriptional activation requires TRRAP and GCN5 cofactors. J. Biol. Chem. *276*, 32627–32634.

Loewith, R., Meijer, M., Lees-Miller, S.P., Riabowol, K., and Young, D. (2000). Three yeast proteins related to the human candidate tumor suppressor p33(ING1) are associated with histone acetyltransferase activities. Mol. Cell. Biol. *20*, 3807–3816.

Lu, X. (1999). Molecular analyses of the class B synthetic multivulva genes of *Caenorhabditis elegans*. PhD thesis, Massachusetts Institute of Technology, Cambridge, Massachusetts.

Lu, X., and Horvitz, H.R. (1998). *lin-35* and *lin-53*, two genes that antagonize a *C. elegans* Ras pathway, encode proteins similar to Rb and its binding protein RbAp48. Cell *95*, 981–991.

McMahon, S.B., Van Buskirk, H.A., Dugan, K.A., Copeland, T.D., and Cole, M.D. (1998). The novel ATM-related protein TRRAP is an essential cofactor for the c-Myc and E2F oncoproteins. Cell *94*, 363–374.

McMahon, S.B., Wood, M.A., and Cole, M.D. (2000). The essential cofactor TRRAP recruits the histone acetyltransferase hGCN5 to c-Myc. Mol. Cell. Biol. *20*, 556–562.

Meijsing, S.H., and Ehrenhofer-Murray, A.E. (2001). The silencing complex SAS-I links histone acetylation to the assembly of repressed chromatin by CAF-I and Asf1 in *Saccharomyces cerevisiae*. Genes Dev. *15*, 3169–3182.

Mello, C.C., Kramer, J.M., Stinchcomb, D., and Ambros, V. (1991). Efficient gene transfer in *C. elegans*: extrachromosomal maintenance and integration of transforming sequences. EMBO J. *10*, 3959–3970.

Miller, L.M., Gallegos, M.E., Morisseau, B.A., and Kim, S.K. (1993). *lin-31*, a *Caenorhabditis elegans* HNF-3/fork head transcription factor homolog, specifies three alternative cell fates in vulval development. Genes Dev. *7*, 933–947.

Osada, S., Sutton, A., Muster, N., Brown, C.E., Yates, J.R., 3rd, Sternglanz, R., and Workman, J.L. (2001). The yeast SAS (something about silencing) protein complex contains a MYST-type putative acetyltransferase and functions with chromatin assembly factor ASF1. Genes Dev. *15*, 3155–3168.

Reifsnyder, C., Lowell, J., Clarke, A., and Pillus, L. (1996). Yeast SAS silencing genes and human genes associated with AML and HIV-1 Tat interactions are homologous with acetyltransferases. Nat. Genet. *14*, 42–49.

Riddle, D.L., Blumenthal, T., Meyer, B.J., and Priess, J.R., eds. (1997). *C. elegans* II (Cold Spring Harbor, New York: Cold Spring Harbor Laboratory Press).

Roth, S.Y., Denu, J.M., and Allis, C.D. (2001). Histone acetyltransferases. Annu. Rev. Biochem. *70*, 81–120.

Saito, R.M., and van den Heuvel, S. (2002). Malignant worms: what cancer research can learn from *C. elegans*. Cancer Invest. *20*, 264–275.

Saleh, A., Schieltz, D., Ting, N., McMahon, S.B., Litchfield, D.W., Yates, J.R., 3rd, Lees-Miller, S.P., Cole, M.D., and Brandl, C.J. (1998). Tra1p is a component of the yeast Ada.Spt transcriptional regulatory complexes. J. Biol. Chem. *273*, 26559–26565.

Sato, T., Russell, M.A., and Denell, R.E. (1983). Homeosis in *Drosophila*: a new enhancer of Polycomb and related homeotic mutations. Genetics *105*, 357–370.

Sigurdson, D.C., Spanier, G.J., and Herman, R.K. (1984). *Caenorhabditis elegans* deficiency mapping. Genetics *108*, 331–345.

Sinclair, D.A., Clegg, N.J., Antonchuk, J., Milne, T.A., Stankunas, K., Ruse, C., Grigliatti, T.A., Kassis, J.A., and Brock, H.W. (1998). Enhancer of Polycomb is a suppressor of position-effect variegation in *Drosophila melanogaster*. Genetics *148*, 211–220.

Solari, F., and Ahringer, J. (2000). NURD-complex genes antagonise Ras-induced vulval development in *Caenorhabditis elegans*. Curr. Biol. *10*, 223–226.

Sternberg, P.W., and Han, M. (1998). Genetics of RAS signaling in *C. elegans*. Trends Genet. *14*, 466–472.

Sternberg, P.W., and Horvitz, H.R. (1986). Pattern formation during vulval development in *C. elegans*. Cell *44*, 761–772.

Sulston, J.E., and Horvitz, H.R. (1977). Post-embryonic cell lineages of the nematode, *Caenorhabditis elegans*. Dev. Biol. *56*, 110–156.

Sulston, J.E., and White, J.G. (1980). Regulation and cell autonomy during postembryonic development of *Caenorhabditis elegans*. Dev. Biol. *78*, 577–597.

Sulston, J.E., and Horvitz, H.R. (1981). Abnormal cell lineages in mutants of the nematode *Caenorhabditis elegans*. Dev. Biol. *82*, 41–55.

Tabara, H., Sarkissian, M., Kelly, W.G., Fleenor, J., Grishok, A., Timmons, L., Fire, A., and Mello, C.C. (1999). The *rde-1* gene, RNA interference, and transposon silencing in *C. elegans*. Cell *99*, 123–132.

Tan, P.B., Lackner, M.R., and Kim, S.K. (1998). MAP kinase signaling specificity mediated by the LIN-1 Ets/LIN-31 WH transcription factor complex during *C. elegans* vulval induction. Cell *93*, 569–580.

Thomas, J.H., Ceol, C.J., Schwartz, H.T., and Horvitz, H.R. (2003). New genes that interact with *lin-35* Rb to negatively regulate the *let-60* ras pathway in *Caenorhabditis elegans*. Genetics *164*, 135–151.

Thomas, J.H., and Horvitz, H.R. (1999). The *C. elegans* gene *lin-36* acts cell autonomously in the *lin-35* Rb pathway. Development *126*, 3449–3459.

von Zelewsky, T., Palladino, F., Brunschwig, K., Tobler, H., Hajnal, A., and Muller, F. (2000). The *C. elegans* Mi-2 chromatin-remodelling proteins function in vulval cell fate determination. Development *127*, 5277–5284.

Whyte, P., Buchkovich, K.J., Horowitz, J.M., Friend, S.H., Raybuck, M., Weinberg, R.A., and Harlow, E. (1988). Association between an oncogene and an anti-oncogene: the adenovirus E1A proteins bind to the retinoblastoma gene product. Nature *334*, 124–129.

Accession Numbers

The GenBank accession numbers for the *mys-1*, *epc-1*, *ssl-1*, and *trr-1* genes are AY551963, AY551964, AY551965, and AY551966.